electronics

MDPI

Article

Energy-Efficient Deployment of Laser Illumination for Rotating Vertical Farms

Tian Liu [1,2], Yunxiang Ye [1,2], Shiyi Tan [1,2], Xianglei Xue [1,2], Hang Zheng [1,2], Ning Ren [1,2], Shuai Shen [1,2] and Guohong Yu [1,2,*]

[1] Institute of Agricultural Equipment, Zhejiang Academy of Agricultural Sciences, Hangzhou 310021, China
[2] Key Laboratory of Agricultural Equipment for Hilly and Mountainous Areas in Southeastern China (Co-Construction by Ministry and Province), Ministry of Agriculture and Rural Affairs, Hangzhou 310021, China
* Correspondence: yugh@zaas.ac.cn

Abstract: As the global population grows, vertical farming offers a promising solution by using vertically stacked shelves in controlled environments to grow crops efficiently within urban areas. However, the shading effects of farm structures make artificial lighting a significant cost, accounting for approximately 67% of total operational expenses. This study presents a novel approach to optimizing the deployment of laser illumination in rotating vertical farms by incorporating structural design, light modeling, and photosynthesis. By theoretically analyzing the beam pattern of laser diodes and the dynamics in the coverage area of rotating farm layers, we accurately characterize the light conditions on each vertical layer. Based on these insights, we introduce a new criterion, cumulative coverage, which accounts for both light intensity and coverage area. Then, an optimization framework is formulated, and a swarm intelligence algorithm, Differential Evolution (DE) is used to solve the optimization while considering the structural and operational constraints. It is found that tilting lights and placing them slightly off-center are more effective than traditional vertically aligned and center-aligned deployment. Our results show that the proposed strategy improves light coverage by 4% compared to the intensity-only optimization approach, and by 10% compared to empirical methods. This study establishes the first theoretical framework for designing energy-efficient artificial lighting deployment strategies, providing insights into enhancing the efficiency of vertical farming systems.

Keywords: vertical farming; artificial lighting; sensor deployment; laser diodes; controlled environment agriculture; differential evolution

Academic Editor: Elias Stathatos

Received: 18 December 2024
Revised: 13 January 2025
Accepted: 14 January 2025
Published: 23 January 2025

Citation: Liu, T.; Ye, Y.; Tan, S.; Xue, X.; Zheng, H.; Ren, N.; Shen, S.; Yu, G. Energy-Efficient Deployment of Laser Illumination for Rotating Vertical Farms. *Electronics* **2025**, *14*, 445. https://doi.org/10.3390/electronics14030445

1. Introduction

The world population is projected to increase from 8.5 billion in 2030 to 9.7 billion by 2050 and 10.4 billion by 2100 [1]. As the population grows, the demand for food production will also increase. Simultaneously, with two-thirds of the global population expected to reside in urban areas by 2050 [2], rapid urbanization places a significant strain on available farmland. To address these challenges, vertical farming has emerged as a promising solution. Using vertically stacked shelves in controlled environments allows efficient crop production within urban areas, reducing dependence on traditional farmland [3].

Light is a crucial factor in plant growth. However, in vertical farming systems, the vertically arranged plant shelves cast shadows on the layers below, significantly reducing light exposure. Studies show that the bottom layer can receive as little as 50% to 10% of the light that reaches the top layer, making light a significant challenge [4] in vertical farming.

As a result, artificial lights are deployed to compensate for the reduced light exposure, but this significantly increases operational costs. Even with energy-efficient options such as light-emitting diodes (LED), lighting expenses account for approximately 67% of the total operating costs [5]. In addition, research on an LED alternative, laser diodes (LDs), has been ongoing since the 1970s [6]. LDs have shown several benefits in agricultural applications, including enhanced seed germination potential [7–9], faster plant maturity [10,11], improved disease resistance [12–14], and increased photosynthetic efficiency [15–18]. More and more vertical farming scenarios are selecting LDs as sources of artificial lights. Despite the advantages, the higher cost of LDs limits their widespread adoption for general lighting in vertical farms.

On the other hand, rotating vertical farms mitigate this limitation by placing shelves in a vertical or horizontal loop that continuously move through conveyor systems (Figure 1). By rotating plants, this system improves the overall light distribution, increasing energy efficiency. Due to the large illumination range of LDs, the number of LDs to deploy is greatly reduced compared to LEDs. In practice, LDs are typically deployed based on empirical methods. **Specifically, the average intensity of the light is the only factor considered, and an LD is placed at the top center of each "V" shaped structure. However, this approach largely overlooks the variations in light intensity and coverage caused by shelf movements, resulting in uneven light distribution.** For example, it can lead to certain layers receiving illumination, while others remain under-illuminated. The unique challenge posed by continuous movement, specifically variations in light exposure, has not been extensively analyzed.

Figure 1. The structure of a rotating vertical farm.

In addition to the light distribution, the movement velocity of rotating vertical farm systems is another critical factor that influences photosynthetic efficiency. Plant photosynthesis responds asymmetrically as plants move in and out of the illumination region. In particular, the photosynthesis rate increases steadily at higher light levels, but declines rapidly as the light intensity decreases [19]. These fluctuations in photosynthesis rates, caused by shelf movement, highlight the importance of rotation velocity. If the velocity is too fast, the exposure time may be insufficient for plants to reach the stable photosynthetic rate, resulting in low light efficiency. To optimize photosynthetic efficiency, the rotation velocity should be calibrated to ensure that the duration of each exposure period allows photosynthesis to stabilize while maintaining even light distribution across all layers throughout the movement cycle.

The above challenges highlight the importance of developing optimized artificial lighting deployment strategies to improve energy efficiency and ensure consistent light

distribution for optimal plant growth in vertical farming systems. Inspired by optimization techniques in sensor deployment, this study addresses the challenges of optimizing artificial lighting deployment in rotating vertical farms by developing a comprehensive strategy to enhance plant growth while reducing energy consumption and operational costs. The first key issue is to model the illumination of LDs, considering factors such as beam patterns and free space loss to characterize the light condition of the target point. Second, a geometric model is developed to characterize the variations in the illuminance area caused by shelf movements. Based on these, a new criterion named cumulative coverage is introduced, quantifying the total illuminance a shelf receives over an entire rotation cycle by integrating coverage area and light intensity over time. Third, the rotation velocity is also taken into account to ensure that the plants maintain a stable photosynthetic rate. Finally, the deployment of LDs for complementary lighting is formulated as an optimization problem with the aim of maximizing cumulative coverage across all shelves. A swarm intelligence algorithm, the Differential Evolution (DE) algorithm, is employed to derive solutions for this complex problem. Experiments are conducted to evaluate the performance of the proposed approach. To our knowledge, this study establishes the first theoretical framework for designing energy-efficient artificial lighting deployment strategies in stacked vertical farming systems, offering novel insights and practical solutions to improve lighting efficiency. The contributions of this paper are threefold.

- **Illumination Strength and Coverage Analysis**: This study examines the illumination strength of LDs, incorporating the beam pattern and free space loss to better understand the variations of the light intensity in different layers. In addition, to characterize the shading effect, a coverage model is established that describes how the coverage area changes as the shelf moves in and out of the illuminance region.
- **Optimization on Novel Criterion**: A new criterion called cumulative coverage is proposed to quantify the total illuminance a shelf receives during a full rotation cycle, in terms of coverage area and intensity, offering a comprehensive measurement of lighting efficiency under the rotation dynamics.
- **Experimental Validation:** Extensive experiments are conducted to demonstrate the technical implementation and effectiveness of the proposed optimization strategy, validating its practical applicability.

The organization of the rest of this paper is as follows: Related work is presented in Section 2. The factors of the illumination strength of the LDs are introduced in Section 3. The light coverage models of the rotating vertical farm are theoretically analyzed in Section 4. The optimization formulation with a novel criterion called cumulative coverage, along with the solution algorithm, are introduced in Section 5. Some numerical simulations and experiments are designed in Section 6 to verify the effectiveness of the proposed deployment method. Conclusions and future work are provided in Section 7.

Throughout this paper, we use the notation in Table 1.

Table 1. Notation and definitions.

Notation	Definitions
l, w, thk	Length, width, and thickness of shelf.
h	Distance between two shelves.
N	Number of vertical layers.
v	Velocity of shelf movement.

Table 1. *Cont.*

Notation	Definitions
ϕ	Angle of chain.
ψ	Pitch angle of light.
θ	Angle of radiation (AoR) of light.
η	Deviation angle.
K^c	Attenuation constant factor of illumination.
K^p	Attenuation primary factor of illumination.
K^q	Attenuation quadratic factor of illumination.

2. Related Work

2.1. Artificial Lighting in Vertical Farming

Light is a critical factor in vertical farming. A combination of blue and red spectra (450–495 and 620–750 nm) in artificial lighting has been evidenced to significantly improve productivity. Extensive research has focused on optimizing light recipes, including the ideal combination of light spectra, duration, and intensity, and how these factors interact with the environment [20–22]. For example, Linn [23] investigated optimal lighting conditions in controlled vertical farming environments, offering experimental recommendations for various crops based on LED technology, photosynthetic photon flux density, crop photoperiods, light color, and overall plant production. Although optimizing light recipes has been a focal point, energy efficiency remains a critical challenge. Kaya et al. [24] highlighted that the exclusive use of artificial light can significantly increase energy consumption. Addressing this, Olvera et al. [25] found that pulsed LED lights, while showing no statistical difference in plant growth compared to continuous LED light, can greatly reduce energy usage. Yalçın et al. [26] explored a solar illumination system with fluorescent coatings, demonstrating that the incorporation of fluorescent reflectors based on optical glass and pigments could significantly improve crop production. Furthermore, Kim et al. [27] developed a crop architecture model using 3D scanning and ray-tracing techniques to better interpret light interception, photosynthetic rate, and light use efficiency. As for rotating vertical farms, Chua et al. [28] explored the light deployment for columnar rotating vertical farm, but only light intensity was considered.

However, most of these studies focus on conventional vertical farming systems with static shelves that ensure uniform light exposure and consistent photosynthetic rates. In contrast, the rotating vertical farms examined in this study differ in two fundamental ways. First, rotating shelves lead to variations in light exposure, affecting both intensity and coverage area, unlike the constant exposure in static systems. Second, as the shelves rotate, photosynthetic rates exhibit asymmetric responses to changing light intensities, whereas in static systems, plants maintain stable photosynthetic rates under constant lighting conditions. The dynamic and automated nature of rotating vertical farms makes them particularly suitable for centralized large-scale plant production. However, the unique challenges posed by continuous movement, specifically variations in light exposure and photosynthetic response, have not been extensively analyzed. There is a notable gap in the literature regarding the optimization of artificial lighting parameters for rotating vertical farms, which this study aims to address.

2.2. Sensor Deployment Optimization

Sensor deployment is a widely studied problem in sensor networks, with applications such as camera placement, light positioning, and base station deployment. The goal of these coverage problems is to effectively monitor a designated target area by strategically deploying sensors. Coverage criteria vary according to task requirements and can include

maximizing the coverage area, ensuring comprehensive coverage without blind spots, and optimizing coverage quality, such as signal strength or data rate.

In the context of camera coverage, the primary objectives are often to maximize the coverage area or to ensure even illumination for high image quality. For example, Lei et al. [29] proposed a visual sensing quality criterion that incorporates factors such as resolution, angle of radiation, focus, occlusion, and relative pose between the camera and the object. This criterion was used to formulate an optimization problem to maximize the target coverage area. In another study, Chen et al. [30] incorporated light reflection and attenuation to optimize the placement of the spotlight in dark indoor settings, with the goal of minimizing the variance in the intensity of the illumination.

In wireless communication networks, the focus shifts to ensuring robust communication links, enhancing coverage, and maintaining network connectivity. For example, Vegni et al. [31] optimized the placement of LEDs in indoor visible light communication systems to balance illumination with reliability of data transmission. Bi et al. [32] studied optimization of the placement of energy and information access points in wireless powered communication networks, optimizing for cost while meeting energy and communication performance standards. Richter et al. [33] studied the effect of micro base station deployment strategies on power consumption in mobile radio networks.

Although these approaches address related optimization challenges, their objectives differ significantly from ours. Sensor network optimization typically focuses on maximizing user coverage, minimizing the number of base stations or access points, or improving metrics such as signal strength and data rate. In contrast, our problem involves optimizing cumulative coverage, a dynamic criterion that is represented as the integral of coverage area and intensity over time. This introduces unique challenges and complexities that are not addressed in traditional sensor network optimization problems.

3. Illumination Strength of LDs

In this section, the illumination strength of LDs is modeled by the beam pattern and free space loss subject to physical properties of LDs.

3.1. Beam Pattern

Conventional light sources often produce non-uniform beam profiles, such as a Gaussian-like distribution, Lambertian distribution, etc. Their spatial distribution can vary depending on the design of the light chip, lenses, and optics. Consider the common Gaussian-like distribution as an example, as shown in Figure 2a. This non-uniform distribution presents challenges in plant illumination due to the central concentration of light that can lead to uneven light distribution, negatively affecting the uniformity of plant growth. To overcome this limitation, optical diffusers can be employed to generate flat-top beams. In contrast to Gaussian beams, flat-top beams offer a more uniform intensity profile, ensuring consistent light distribution over the entire target area. This characteristic makes flat-top beams highly beneficial for plant illumination applications where even light exposure is essential. A comparison between Gaussian and flat-top beams is depicted in Figure 2.

While optical diffusers effectively scatter light in the central area, intensity decreases towards the edges. This attenuation effect becomes more noticeable as distance increases, making the deviation angle a critical factor in maintaining consistent illumination across a given area. Therefore, we define the angle of radiation (AoR) of an LD as the angular range where the laser light maintains uniform intensity. AoR is represented by θ and can be visualized in Figure 3. Let η be the deviation angle between the target point P and

the central direction of the light source **n**. Inspired by [30], a flat-top beam pattern can defined as follows:

$$I^{AoR}(P) = \begin{cases} 1 & 0 \leq \eta \leq \theta/2 \\ 0 & \text{otherwise.} \end{cases} \tag{1}$$

The deviation angle η can be calculated by

$$\eta = \arccos \frac{-\mathbf{n} \cdot \vec{SP}}{\|\mathbf{n}\| \|\vec{SP}\|}. \tag{2}$$

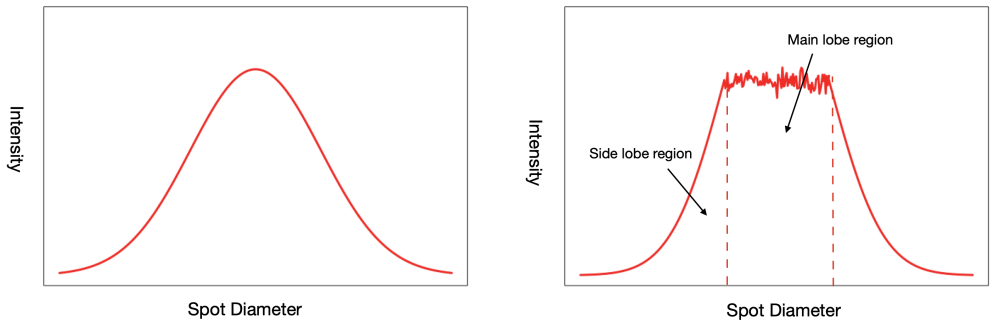

(**a**) (**b**)

Figure 2. Experimental irradiance profile of a Gaussian beam (**a**) and a flat-top beam (**b**).

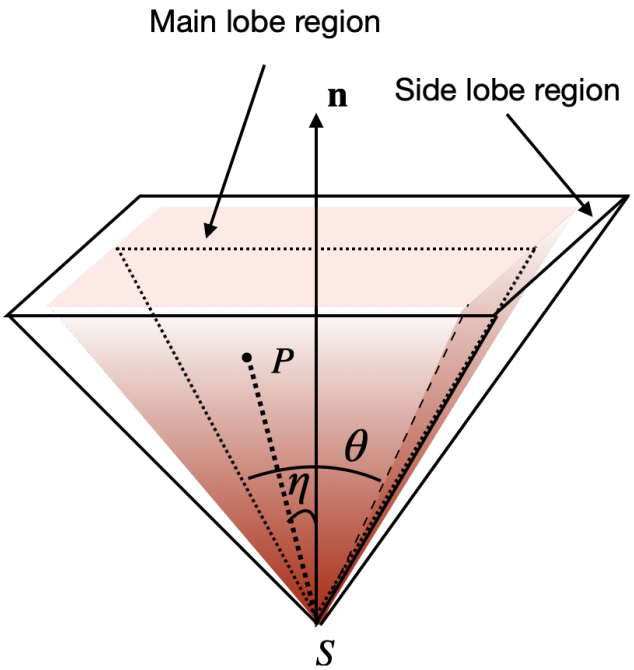

Figure 3. Geometrical illustration of beam pattern of LDs.

Free Space Loss

Free space loss is the decrease in light intensity as the distance from the source increases. This phenomenon follows the Inverse Square Law, which indicates that light intensity

diminishes in proportion to the square of the distance from the source. As provided by [30], the attenuation can be mathematically represented as follows:

$$I^{FSL}(d) = \frac{1}{K^q \cdot d^2 + K^p \cdot d + K^c}, \tag{3}$$

where K^q, K^p, and K^c are the quadratic, primary, and constant attenuation factors, respectively. The constant attenuation factor K^c is necessary and is often set to 1, ensuring that the illumination is strongest at the light source and attenuates with increasing distance. $d = \|\vec{SP}\|$ is the Euclidean distance between the light source S and target point P. $I^{FSL}(\cdot)$ is a monotonically decreasing function of distance d, satisfying $I^{FSL}(0) = 1$ and $\lim_{d\to\infty} I^{FSL}(d) = 0$.

Figure 4 depicts the light intensity at different spatial locations. The color spectrum reflects the intensity levels, with red denoting high intensity and blue indicating low intensity. The beam exhibits a pyramid-like shape, with the highest intensity concentrated at the light source. Points sharing identical horizontal coordinates exhibit uniform intensity levels. The parameters are set as $K_c = 1, K_p = 0.45, K_q = 0.75$. The intensity decreases as the distance from the light source increases, with the most significant drop occurring near the source (shown in Figure 5).

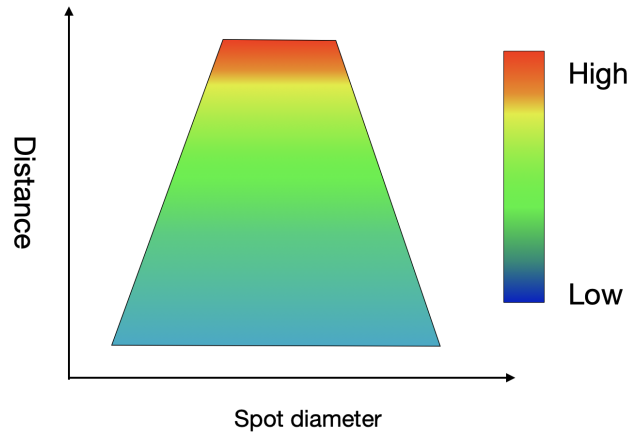

Figure 4. Two-dimensional illustration of spatial intensity distribution.

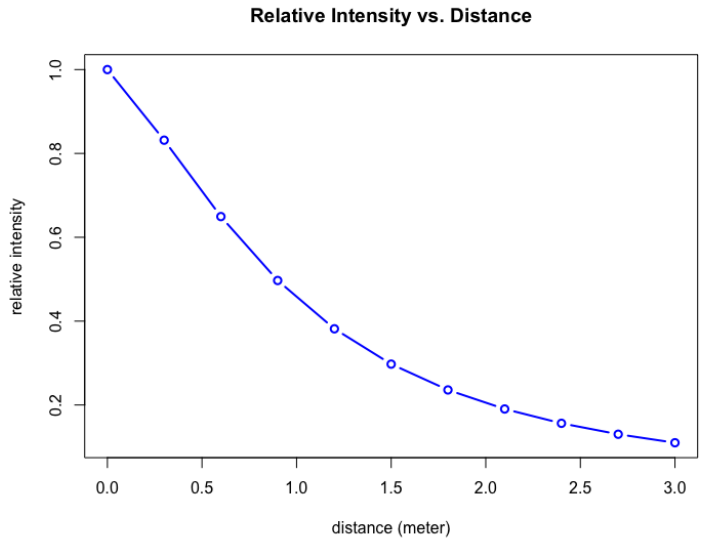

Figure 5. The relationship between intensity and distance to the light source.

3.2. Illumination Strength of LDs

To determine the illumination of a target point, we define illumination strength based on the AoR and free space loss, which can be formulated as

$$L_P = L_S \cdot I^{FSL}(d) \cdot I^{AoR}(\eta), \tag{4}$$

where L_S is the initial intensity produced by the laser source S. $I^{FSL}(d)$ is the illumination attenuation due to free space loss over distance d, while $I^{AoR}(\eta)$ denotes the angle-dependent illumination change concerning deviation angle η.

4. Coverage Models of the Rotating Vertical Farms

4.1. Simplified Model of the Rotating Vertical Farm

The rotating stacked farm is a complicated system that consists of the following core parts: (1) Central Structure: The central structure serves as the pivot point of the entire system. This sturdy central structure enables the rotation of the stacked layers. (2) Stacked Layers: The farm comprises multiple horizontal shelves, arranged vertically by chains, forming multiple "V" shapes. These layers hold plant containers or trays, which are typically rectangular. Each layer, with a width w, length l, and a vertical separation h from the neighboring layers, is stacked vertically N times. (3) Rotating Mechanism: A motorized rotation mechanism is used that gently rotates the stacked layers to evenly distribute light and nutrients for optimal growth conditions. The angular difference of the chain and the vertical is denoted as ϕ, while the layers move along the chain with velocity v.

The aim of this study focuses primarily on the variations in the illumination coverage area, light intensity, and their influence on overall photosynthesis when coupled with the rotation velocity. In the previous section, we found that the beam pattern of an LD forms a four-sided pyramid (shown in Figure 3), and the light intensity is only related to the deviation angle and the distance to the light source. Therefore, the deployment of light sources can be studied in a 2D model of a rotating vertical farm system, as illustrated in Figure 6.

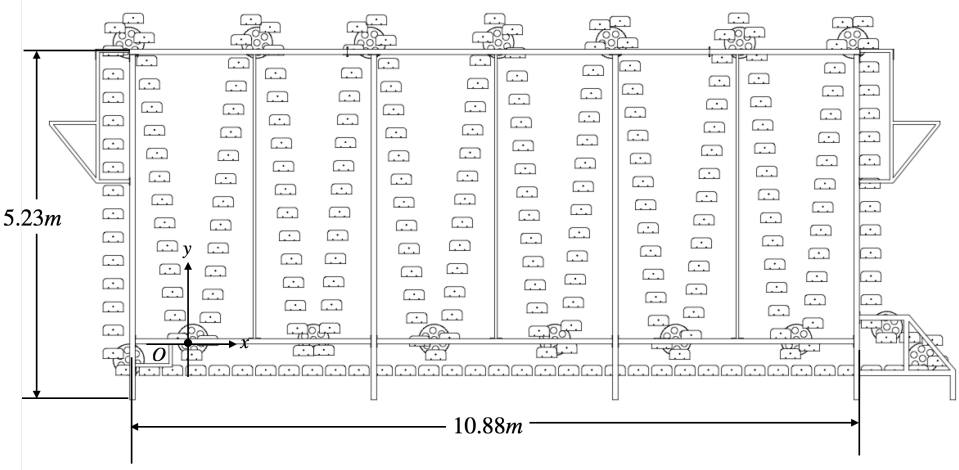

Figure 6. Vertical rotating farm in 2D view.

Other than this, the positions of a light source usually comprise the spatial coordinates and orientations, i.e., pitch, yaw and roll. However, including all three angles would unnecessarily complicate the problem without significantly improving its effectiveness. Examining the orientations in this deployment scenario more closely, the pitch angle determines the angle at which light is projected relative to the vertical direction of the plants, which significantly affects the intensity and uniformity of light received. In contrast,

the yaw and roll angles are related to horizontal directions and have minimal influence on the vertical coverage of light on plants. Therefore, we focus only on optimizing the pitch angle and exclude the yaw and roll angles from consideration in the optimization. The position parameters to be optimized are defined as follows. Assume M lasers are employed to perform the illumination task. Denote $\mathbf{LD}_i = [x, y, \psi]^T \in \mathcal{R}^3$ ($i \in [M]$) as the position parameters of the i-th LD, where $[x, y]$ gives the spatial coordinates, and $\psi \in [0, \frac{\pi}{2}]$ is the pitch angle. The above simplifications significantly reduce computational complexity, enabling more efficient optimization while maintaining accuracy and effectiveness.

4.2. Coverage Models

To precisely examine the dynamics of the illuminated area, we categorize the coverage into three stages, depending on how the layers move in relation to the illuminated region:

1. **Entering the Illuminated Zone**: As the layers rotate in the illuminated zone, the coverage area gradually increases.
2. **Maintaining Coverage**: After complete entry into the light zone, the coverage stays constant for a period.
3. **Exiting the Illuminated Zone**: As the layers rotate out of the illuminated zone, the coverage area decreases until illumination diminishes.

This three-stage framework allows for a precise analysis of how light coverage fluctuates based on the rotation of the layers within the stacked farm. The following part will explore these stages in depth to understand how the coverage area changes.

The Entering Stage

The geometrical relationship between the light source and the layers is illustrated in Figure 7. Denote the coordinates of the light source as $S = (S_x, S_y)$. Layers move along the chain with velocity v. The angle between the chain and the vertical axis, measured counterclockwise, is denoted by ϕ. The coordinate system is constructed based on the movement trajectory of point A. Specifically, the origin O of the coordinate system is defined at the initial point of A. x and y represents the coordinates of point A, as shown in Figure 6. Based on this setup, the movement of point A can be mathematically represented as a straight line:

$$y = x \cdot \tan\phi + b, \tag{5}$$

where b is the interception. Incorporating the shading effect resulting from the stacked structure, the essential points of focus are specified as follows:

- $A(t)$: The upper-right vertex of the layer at time t.
- $B'(t)$: The lower-right vertex of the layer directly above, primarily responsible for the shading impact.
- $B(t)$: The intersection of SB' with the lower layer.

The first step to calculate the coverage area is to determine if a target point lies within the illumination region. A point P is defined to be within the illumination region if it satisfies the following conditions:

1. **Position Relative to the Start Arm**: The point P must lie counterclockwise relative to the start arm of the sector.
2. **Position Relative to the End Arm:** The point P must lie clockwise relative to the end arm of the sector.
3. **Distance Constraint** (optional): The Euclidean distance between the target point P and the light source S must be less than the coverage radius r. That is, $\|SP\| \leq r$.

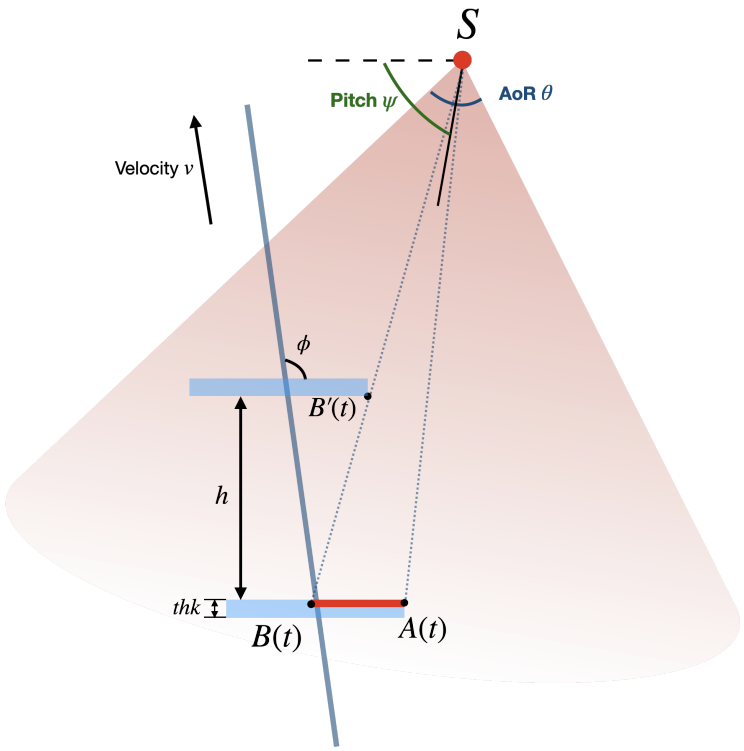

Figure 7. An illustration of the entering stage.

The detailed algorithm can be found in Algorithm 1.

Algorithm 1 Check if a given point is inside a sector.

Input: light source (S_x, S_y), point (P_x, P_y), pitch angle ψ, angle of radiation θ, coverage radius r.
Output: if point P is inside the coverage region of S.

1: The slope of the start and the end arm is $k_1 = \tan(\psi - 0.5\theta)$ and $k_1 = \tan(\psi + 0.5\theta)$, respectively.
2: Two straight lines will form two sector-shaped regions. The one where the illumination is directed toward the bed is kept.
3: The interception of each arm is calculated as $b_1 = S_y - k_1 \cdot S_x$ and $b_2 = S_y - k_2 \cdot S_x$.
4: Calculate the distance of point P to S, $d = \|\vec{SP}\|$.
5: The vector of the start arm $\vec{v_1}$, the vector of the end arm $\vec{v_2}$, and the vector of $\vec{SP}$.
6: Find the normal vector of $\vec{v_1}$ and $\vec{v_2}$ as $\vec{n_1}$ and $\vec{n_2}$.
7: **if** $d < r$ (optional) **and** $\vec{n_1} \cdot \vec{SP} < 0$ **and** $\vec{n_2} \cdot \vec{SP} \geq 0$ **then**
8: Point P is in the coverage region.
9: **end if**

Next, we determine the coverage area by applying geometric principles. Since the laser beam is focused and directional without dispersing into multiple directions, we only consider the direct transmission of light and ignore the reflection and scattering.

When a layer enters the illuminated region, the coverage area is decided by $A(t)$ and $B(t)$. The following calculates the movement and positions of these functions:

- **Point** $A(t)$: Point $A(t)$ moves along the straight line $y = x \cdot \tan\phi$ as the layer rotates. The coordinate of $A(t)$ at time t is

$$A(t) = (A_x(t), A_y(t)) = (vt \cdot \sin\phi, vt \cdot \cos\phi). \tag{6}$$

- **Point** $B'(t)$: The lower-right vertex of the layer above onto the current layer, has the following coordinates:

$$B'(t) = (A_x(t) + h \cdot \tan\phi, A_y(t) + h + thk). \quad (7)$$

- **Point** $B(t)$: Point $B(t)$ is the intersection of $\vec{SB'}$ and the current layer. The horizontal coordinate of $B(t)$ is determined by the intersection of the line $\vec{SB'}$ and $x = A_x(t)$. It shares the same vertical coordinate as $A(t)$.
- **Coverage Area Formula:** When point $A(t)$ enters the illuminated zone, the coverage area is calculated by

$$Area_1(t) = abs(A_x(t) - B_x(t)). \quad (8)$$

The detailed algorithm can be found in Algorithm 2.

Algorithm 2 Calculation of coverage area of the entering stage.

Input: light source $S = (S_x, S_y)$, height between two layers h, angle of the chain ϕ, thickness thk.

1: Assume the initial point of $A(t)$ is the origin O, its coordinate can be represented as $(A_x(t), A_y(t)) = (vt \cdot \sin\phi, vt \cdot \cos\phi)$.
2: The coordinate of $B'(t)$ can be represented by $(A_x(t) + h \cdot \tan\phi, A_y(t) + h + thk)$.
3: The slope of line $SB(t)$ can be calculated by $k = (S_y - B'_y(t))/(S_x - B'_x(t))$, and the interception can be calculated by $b = B'_y(t) - k \cdot B'_x(t)$.
4: The coordinate of $B(t) = ((A_y(t) - b)/k, A_y(t))$.
5: **return** The coverage area is $Area_1(t) = abs(A_x(t) - B_x(t))$.

4.3. The Maintaining Stage

As the layers move, the upper layers may no longer block the light, allowing the lower layers to be completely illuminated, as shown in Figure 8. During this stage, the shading effect from the upper layers is no longer a factor, and the illuminated area remains constant, which is the width w of the layers with the following formula:

$$Area_2(t) = w, \text{ if } abs(A_x(t) - B_x(t)) > w. \quad (9)$$

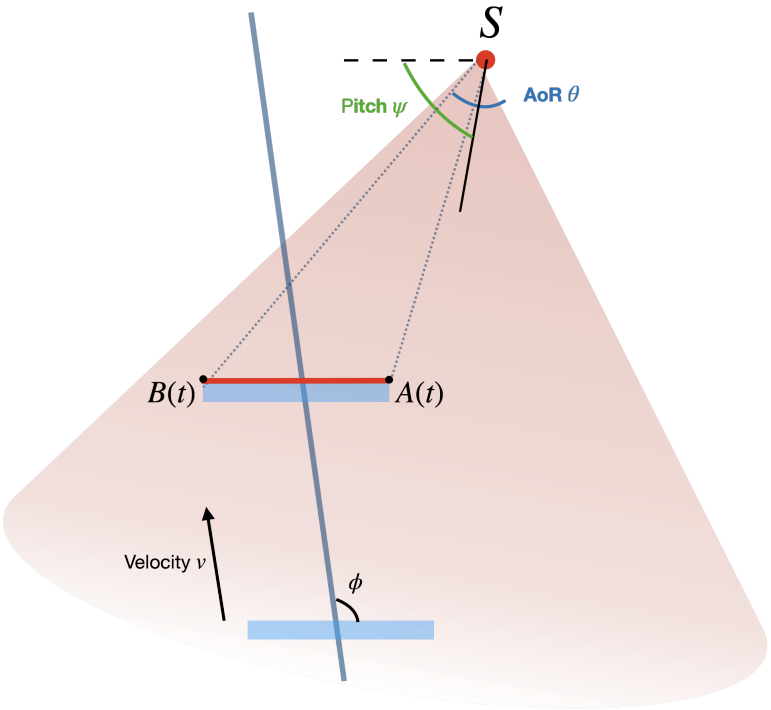

Figure 8. An illustration of the maintaining stage.

4.4. The Exiting Stage

As the layer moves out of the illumination region, the coverage area gradually decreases. As illustrated in Figure 9, this stage begins as the upper right point of the layer, $C(t)$, moves out of the illuminated region. Let $C'(t)$ represent the point where the layer intersects with the boundary of the illuminated region. Here we describe how to calculate the coverage area for the exiting stage.

- Since $C'(t)$ and $A(t)$ share the same coordinate y, the coordinate x of $C(t)$ can be calculated by finding the intersection of the layer and the boundary of the illumination region. Assume that the boundary that intersects the layer has slope k_1 and intercept b_1, the coordinate of $C'(t)$ is as follows:

$$C'(t) = ((A_x(t) - b_1)/k_1, A_y(t)). \tag{10}$$

- **Conditions for Coverage Area Calculation:** During this stage, $C(t)$ is checked to ensure it is outside the illuminated area, while $A(t)$ remains inside. This condition indicates that the coverage area is shrinking as the layer exits the illuminated region.
- **Coverage Area Calculation:**

$$Area_3(t) = abs(C'_x(t) - A_x(t)). \tag{11}$$

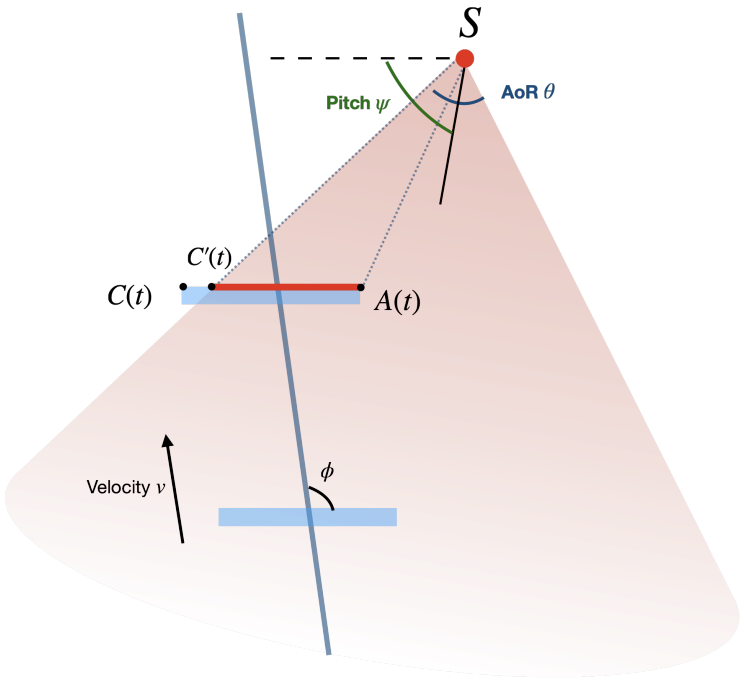

Figure 9. An illustration of the exiting stage.

It is crucial to understand that the movement of layers within the illuminated area may not consistently cover all three coverage stages, and the variation of coverage exhibits different patterns, as shown in Figure 10. Note that the farm system is simplified into a 2D view. In this context, the movement and positions of the light sources directly influence the width of the coverage area. As a result, the width is considered equivalent to the coverage area. Several factors may contribute to this uncertainty, such as the initial position of the layer, the position of the light source, and the beam pattern of the lights. These factors can result in different coverage behaviors based on the system setup and dynamics. For instance, if the Angle of Radiation (AoR) is small and the layers are wide, only the edges of

the layer receive illumination, leaving the central area under illuminated. In such cases, the entire layer is not illuminated before transitioning to the exiting stage.

Furthermore, depending on the configuration and velocity of movement, some layers may not progress evenly through all stages. For example, with a small pitch angle of the light source, the duration of the exiting stage is significantly reduced, leading to a rapid decrease in the coverage area to zero. This variability highlights the need for adaptable models that can effectively depict the dynamic coverage nature in vertical rotating farms. By accounting for these complexities, such models are significant in ensuring optimal light exposure, even under varying conditions.

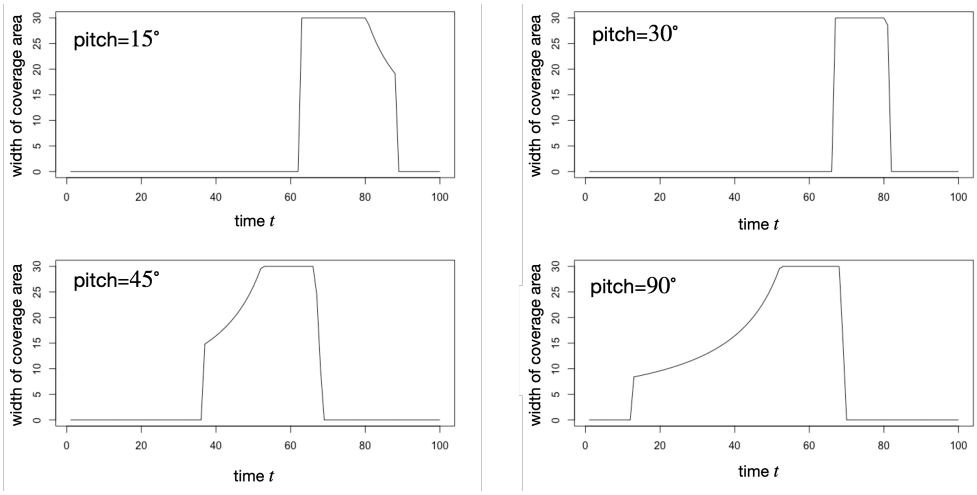

Figure 10. Coverage patterns under various parameter settings as the layer moves along one side of the "V" shape of the rotating vertical farm.

5. Optimization

5.1. Optimization Formulation

The main objective of this work is to deploy a number of LDs such that illumination efficiency is maximized. Existing approaches or practices primarily focus on light intensity when determining the positions of light sources, but they often overlook shading effects, which significantly impact overall illumination performance. Therefore, we propose a new criterion, called cumulative coverage, which considers both intensity and coverage area. Let $\Lambda = \{\mathbf{LD}_1, ..., \mathbf{LD}_M\}$ be the set of positions of M lights. Let $P \in \Omega$ denote the target point to be covered, and Γ denote the velocity range. The cumulative coverage is defined as follows:

$$\mathcal{H}(\mathbf{LD}_1, ...\mathbf{LD}_M, P, v) = \int_0^T (Area(t) + Area_2 + Area_3(t)) \cdot L_p(t) \tag{12}$$

Mathematically, it is the integral of $Area(t) \cdot L_p(t)$ over the total operating time T, where the T is measured in seconds, $Area(t)$ is measured in cm^2 and $L_p(t)$ is a scalar representing the relative illumination strength relative to the light source. Therefore, with the given target and laser lights, the deployment optimization problem for coverage can be formulated as

$$\arg\min_{LD_1,...LD_M,v} \mathcal{H}(\mathbf{LD_1}, ...\mathbf{LD_M}, P, v) \tag{13}$$

$$\text{s.t. } \mathbf{LD} \in \Lambda, P \in \Omega, v \in \Gamma. \tag{14}$$

Here, we provide a visual illustration of the illumination for regular farms and rotating vertical farms in Figure 11. Assume that the intensity of the light source is 1, and the width of the layer is 30. The light is deployed in the top center of the "V" shaped structure.

The red dotted line represents the illumination condition in regular farms, where each point receives even illumination. The solid blue line represents the illumination status, as a single layer completes the movement along an entire "V" shape. Focusing on the motion of the layer along one side of the "V" shape, it first enters the illuminated region, where it receives high light intensity. As the layer descends, the light intensity gradually decreases as a result of free space loss. Eventually, the layer exits the illuminated region and reaches the bottom of the "V" shape. The process is mirrored on the other side of the "V" shape.

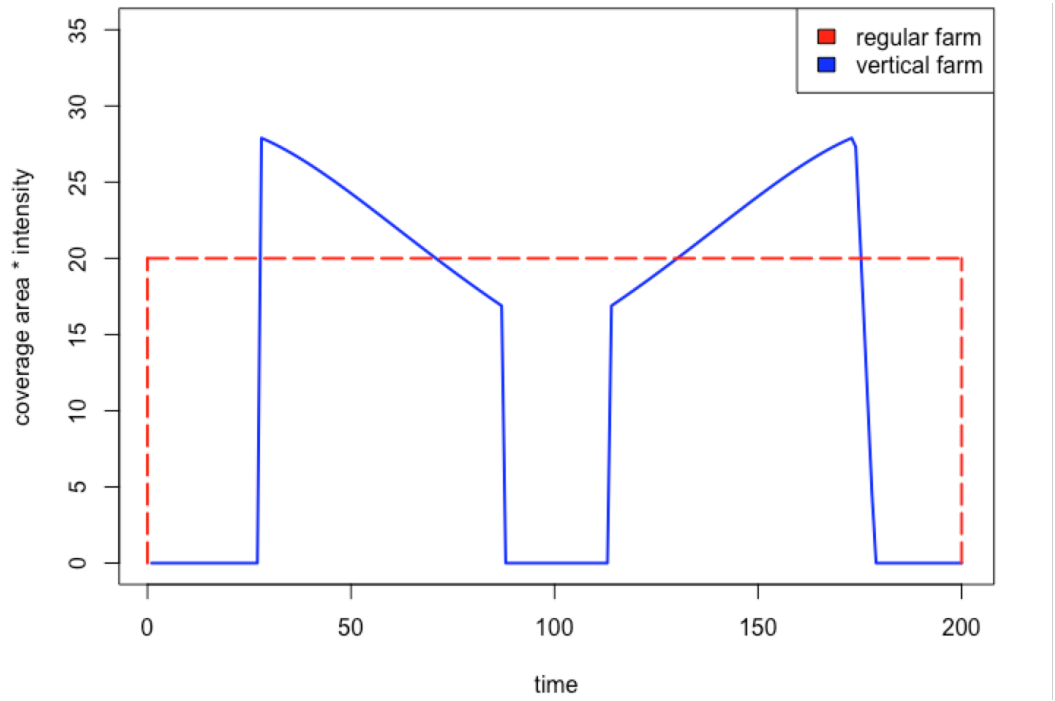

Figure 11. Illustration of illumination difference between regular farm and rotating vertical farm.

5.2. Optimization Algorithm

The goal of optimization is to find the position parameters, i.e., $[x, y, \psi]$, that maximize the criterion proposed in Equation (13), which considers both intensity (Section 3) and shading effect (Section 4). To solve this problem, we adopt a population-based stochastic optimization algorithm for several key reasons. First, the parameters to be determined, that is, spatial positions $[x, y]$, pitch angle ψ, and velocity v, differ in meaning and units, making normalization between variables challenging. Second, the search space for light positions consists of multiple potential deployment location sets. Other algorithms, such as gradient-based algorithms, struggle to handle such constraints effectively, often leading to violations. Lastly, the objective function is non-differentiable, rendering gradient-based methods unsuitable for this optimization task.

For these reasons, we employ the Differential Evolution (DE) algorithm, introduced by Storn and Price in 1996 [34]. DE is a robust, population-based optimization technique that is well suited to non-linear, non-differentiable problems. The DE algorithm optimizes the solution iteratively through the following steps: (1) The initial population of candidate solutions is randomly generated within the variable bounds. Each candidate represents a potential configuration of light positions, poses, and velocities. (2) In each generation, a mutant vector is created by combining a target vector (parent) with the weighted difference of two randomly selected variables from the population. This introduces diversity and explores the search space effectively. (3) The mutant vector is then combined with the target vector to form a candidate solution (offspring). This step ensures variability while retaining key characteristics of the parent. (4) A comparison is made between the

parent and the offspring. The better performing solution is retained for the next generation, ensuring continuous improvement.

The use of DE has the following advantages: (1) **Increased likelihood of finding global optimum:** The diversity introduced by mutation and crossover reduces the risk of the solution getting trapped in local optima, improving the probability of finding the global optimum [34]. (2) **Adaptability for various deployment tasks:** DE easily adapts to different deployment requirements. For example, in this study, we specify the number of lights to be deployed and allow DE to identify optimal placements. This adaptability also allows DE to handle related tasks, such as determining the optimal number of lights or minimizing installation and operational costs.

Since lights can only be installed in specific spaces, such as within the inner space of the "V" shaped structure, a constraint handling method is required to ensure the feasibility of output positions. We employ a heuristic approach in which a constraint check is performed each time a new individual is generated. Any offspring that does not meet the constraint is discarded. The pseudocode for the modified DE is presented in Algorithm 3.

Algorithm 3 DE algorithm

Input: GEN_{MAX} {maximum number of generations}, NP {population size}, f {objective function}, CR {crossover rate}, F {mutation rate}.
Output: position vector $\mathbf{x}$

$g = 0$
Population initialization $\mathbf{x}_{i,0}$ for $i = 1, ..., NP$.
Evaluate the $f(\mathbf{x}_{i,g})$ for $i = 1, ..., NP$.
for $g = 1 : MAX_{GEN}$ **do**
  for $i = 1 : NP$ **do**
    Randomly select r_1 and r_2.
    for $j = 1 : D$ **do**
      if $(rand_j[0, 1) < CR$ **then**
        $\mathbf{u}^j_{i,g+1} = \mathbf{x}^j_{best,G} + F(\mathbf{x}^j_{r_1,g} - \mathbf{x}^j_{r_2,g})$
        Consistently check if the offspring $\mathbf{u}_{i,g+1}$ satisfies the constraints or not; discard the offspring that fails to meet the constraint.
      else
        $\mathbf{u}^j_{i,g+1} = \mathbf{x}^j_{i,G}$
      end if
    end for
    Evaluate $f(\mathbf{u}_{i,g+1})$
  end for
end for

6. Simulation

In this section, simulations for deploying LDs for optimal illumination coverage are carefully designed, and the effectiveness of the proposed approach is demonstrated by analyzing the results.

6.1. Simulation Settings

As shown in Figure 6, a rotating vertical farm consisting of six "V" shaped structures is chosen as the target. Suppose that the layers are composed of the same material, whose intrinsic parameters are shown in Table 2. The simulation was performed using R version 4.4.2.

We define the spatial constraints for the lights to be within the "V" shaped structure and set the number of light equal to the number of "V" shaped structure, which is six in this case, for the following reasons. First, the upper part of the system receives sufficient sunlight, while the lower part of the structure experiences insufficient light. Installing

lights within "V" shaped structures maximizes their effectiveness. Additionally, these constraints ensure that the solution adheres to the geometric and practical limitations of the system. In addition, as the layers traverse all the "V" shaped structures, they cycle back to the starting point through the lower part of the farming system, where space is limited, and light efficiency is significantly reduced. Therefore, the number of lights is set to six, with the focus placed exclusively on the layers within the "V" shaped structures to achieve optimal illumination.

Table 2. Values of lights and rotating farms.

Description	Parameter and Value
Intensity reference value	$I = 1$
AoR	$\theta = 100^{\circ}$
Attenuation quadratic factor	$K^q = 0.075$
Attenuation primary factor	$K^p = 0.045$
Attenuation constant factor	$K^c = 1$
Width and thickness of shelf	$w = 30$ cm, $thk = 2$ cm
Distance between two layers	$h = 38$ cm
Number of layers	$N = 14$
Angle of chains	$\phi = 96.35^{\circ}$ or $\phi = 83.65^{\circ}$
Movement velocity	$v = 0.015$–0.26 m/s

Furthermore, only direct light transmission is taken into account while reflection is ignored for the following reasons: (1) In total, 80–90% of the light can be absorbed by plants. (2) The light source positioned above causes the reflected light to typically travel in a direction opposite to the incoming light. This phenomenon can effectively hinder reflected light from reaching the tops of plants that are growing upward.

6.2. Impact of Single Variable on Coverage Area

We first examine the relationship between the coverage area and different values of pitch angle, velocity, and AoR.

6.2.1. Relationship Between Pitch Angle and Coverage Area

We begin by examining how pitch affects the coverage area for one "V" shaped structure. In this experiment, the LDs are placed in the top center of the "V" shaped structure, with varied pitch angles. The velocity of movement is fixed at 10 cm/s. Since the structure is symmetric, we plot the cumulative coverage against the pitch angle for two scenarios: (1) The layers only move along one side of the "V" shape. (2) The layer moves along the entire "V" shape. In Figure 12a, the cumulative coverage is recorded as the layer moves along one edge of the "V" shaped path. The cumulative coverage increases rapidly with the pitch angle, reaching a maximum of approximately 40° to 50°. Beyond this range, the cumulative coverage begins to slowly decline. In Figure 12b, we examine the cumulative coverage as the layer moves along both edges of the "V" shape. Here, the cumulative coverage increases monotonically, reaching its maximum when $\psi = 90^{\circ}$. In particular, the slope is steepest between 40° and 50°, indicating this range as a critical transition point where coverage efficiency changes most rapidly.

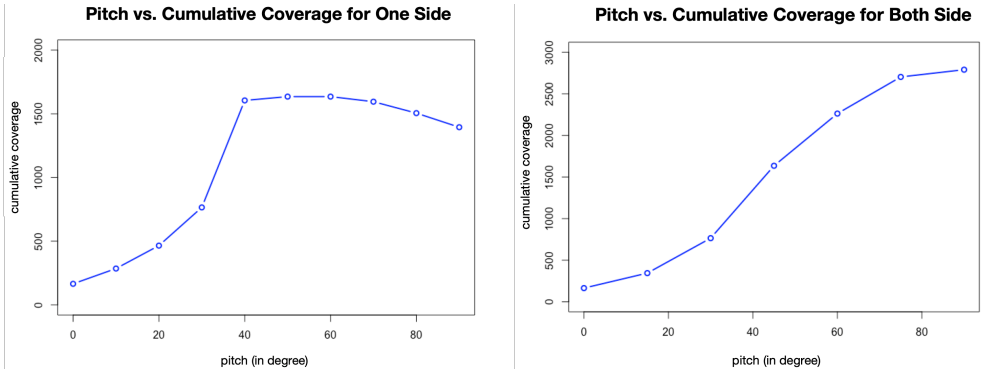

(**a**) One side. (**b**) Both sides.

Figure 12. The relationship between pitch and cumulative coverage for one side and both sides.

6.2.2. Relationship Between Velocity and Coverage Area

According to [19], plants dynamically adjust to the change in light to optimize photosynthesis. In the rotating vertical farm system, rotation leads to fluctuations in the photosynthesis rate. Although photosynthesis generally increases with light intensity, plants do not react to sudden exposure instantly. Instead, upon exposure, the photosynthetic rate gradually reaches a stable level, with the final rate differing depending on the light condition. Typically, the stabilizing time is 15 min and 30 min for limited light or saturated light, respectively. In contrast, when transitioning from saturated to limited light, the photosynthetic rate presents two patterns according to the plant types. For species like soybeans and rice, it initially declines sharply to a low level, then gradually rises to stability, as illustrated by the dotted line in Figure 13. In contrast, for other species such as wheat and pumpkin, the rate drops directly to the stable value [19], as represented by the solid line in Figure 13.

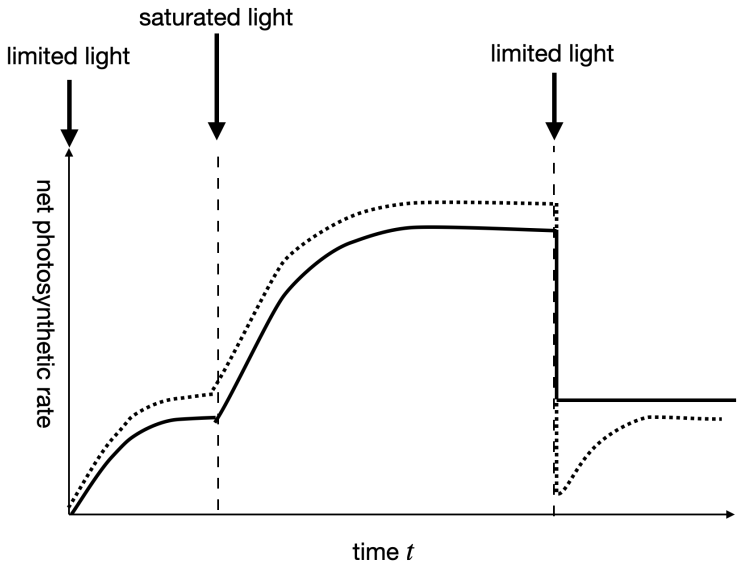

Figure 13. Two types of plant photosynthetic responses to changes in light intensity.

The observations highlight an important point. When the movement velocity is too fast, plants often alternate between illuminated and under-illuminated regions, leading to a reduction in their overall photosynthetic efficiency. To promote growth, it is recommended to set the velocity of movement such that plants have adequate time to maintain a consistent photosynthetic rate.

In this experiment, the laser diode is placed in the top center of the "V" shaped structure, with the pitch angle set to $\psi = 90^\circ$ and the AoR set to $\theta = 90^\circ$. The velocity

of movement v varies from 2 cm/s to 20 cm/s. We analyze the cumulative coverage for different velocities, as shown in Figure 14. Two metrics are considered: the cumulative coverage during one complete movement cycle and the cumulative coverage in unit time. In Figure 14a, the cumulative coverage jumps to the maximum when v = 4 cm/s. Beyond this point, the coverage area gradually decreases as velocity increases. This occurs because as the velocity increases, the layers spend less time within the illuminated region. However, when analyzing the cumulative coverage per unit time, the cumulative coverage remains relatively stable for velocities of $v \geq 6$ cm/s.

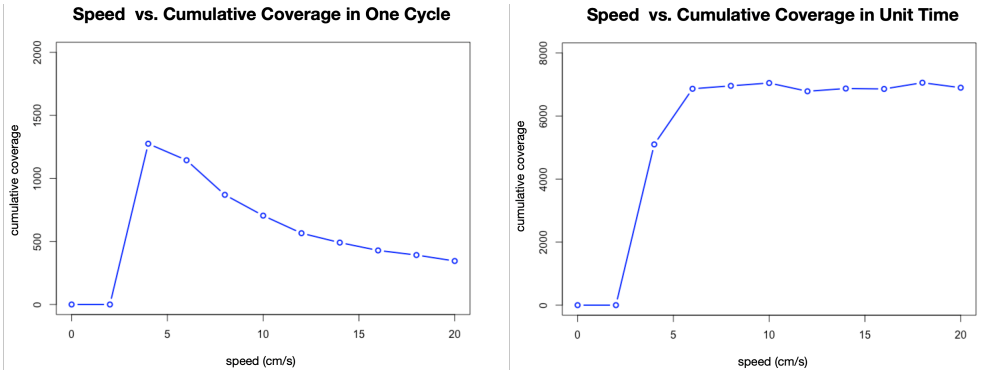

(**a**) In one cycle. (**b**) In unit time.

Figure 14. The relationship between layer movement velocity and cumulative coverage size.

As the above phenomenon indicates that consistent light exposure enhances photosynthetic efficiency, a slower movement velocity is preferred to maximize the duration of illumination. In addition, a pause can be introduced to let the plant maintain a stable photosynthetic rate. When the layers reach the top of the farm, where the lights transition from artificial to natural light, this consistent exposure helps to maintain a high net photosynthesis rate, optimizing the overall impact of artificial lighting.

6.2.3. Relationship Between AoR and Coverage Area

Next, we examine how the AoR of the LDs affects the coverage area. In this experiment, the laser diodes are positioned in the top center of the "V" shaped structure, with the AoR θ varying from 90° to 150°. The movement velocity is fixed at 10 cm/s and the pitch angle is set to 90°. The cumulative coverage is plotted against different AoR values, as shown in Figure 15. The results indicate a linear relationship between the AoR and the cumulative coverage. While a larger AoR provides a greater cumulative coverage—e.g., an AoR of 150° increases the cumulative coverage by 14% compared to 90°—this comes at a cost. Wider AoRs typically require more expensive hardware and also lead to higher operating costs due to increased power consumption.

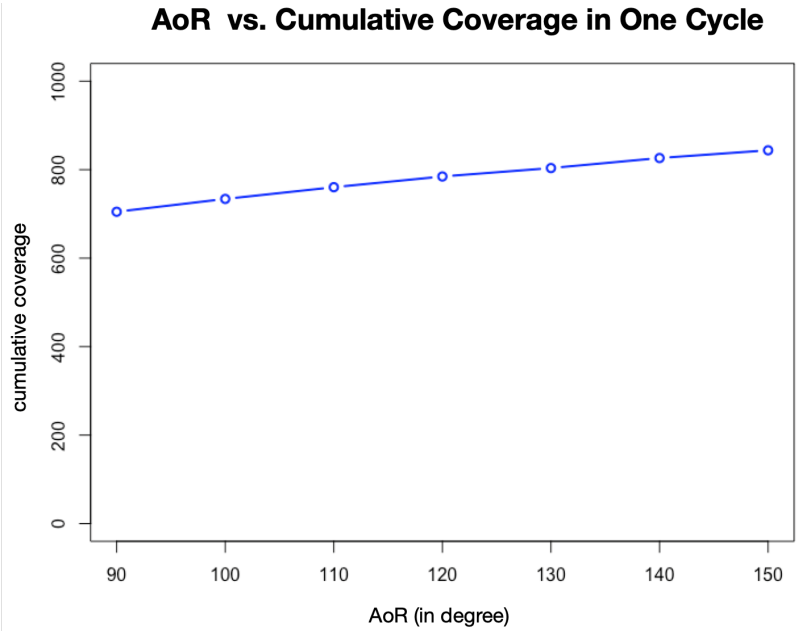

Figure 15. The relationship between AoR and cumulative coverage.

6.3. Overall Comparison

The position parameters to optimize include the spatial coordinates and pitch angles of the LDs. These parameters are adjusted to meet plant-specific light requirements while satisfying practical constraints. To validate the effectiveness of the proposed approach, we compare the proposed optimization strategy with three alternative approaches.

- **Setting 1: Optimization of the proposed cumulative coverage:** This strategy focuses on maximizing cumulative coverage over time, considering both the coverage area and the light intensity.
- **Setting 2: Optimization of the proposed cumulative coverage with variable height only:** Empirically, the light is placed in the upper center of the "V" shaped structure and the pitch angle is usually fixed at 90°. This optimization focuses solely on the adjustment of the height.
- **Setting 3: Empirical method on average intensity:** This strategy is representative of most practical scenarios, where the position of the light source is determined based on the average intensity across layers. Specifically, it performs a random search, measures the average intensity of each layer for each search position, and selects a position that has the highest average intensity. The best value is recorded over 100 search times.
- **Setting 4: Optimization on Desired Intensity:** This approach accounts for the light compensation point (LCP) of plants, e.g., 20–50 μmol m^{-1} s^{-1} for rice (*Oryza sativa* L.) [35]. It ensures that the cumulative coverage is calculated upon the minimum required threshold for photosynthesis. By maintaining light levels above the LCP, this strategy supports plant energy needs and promotes healthy growth.

We let the layer complete the movement of the entire "V" shaped structure and record the corresponding metrics. The parameters of the DE algorithm are set as follows: The size of the population NP, the crossover rate CR, the probability of mutation F, and the termination condition GEN_{max} are set to 100 iterations. The parameter values are shown in Table 3.

Table 3. Parameters of DE.

Description	Parameter
Population size	$NP = 20$
Mutation probability	$F = 0.7$
Maximum number of generations	$GEN_{max} = 100$
Crossover rate	$CR = 0.5$

We record the optimal light positions, including the spatial coordinate (S_x, S_y) and the pitch angle. We also record the optimal objective values, in terms of the proposed criterion. The experimental results are shown in Table 4.

Table 4. Comparison of deployment performance for 4 different settings.

AoR (°)	S_x	S_y	Pitch (°)	Optimal Cumulative Coverage
Setting 1: Ours				
80	3.77	299	87.08	1373
90	4.01	292	85.37	1437
100	−5.16	281	96.26	1500
110	−6.26	275	96.83	1545
Setting 2: Ours on Height Only				
80	Fixed with 0	293	Fixed with 90	1307
90		283		1375
100		269		1438
110		266		1509
Setting 3: Empirical Method				
80	Fixed with 0	275	Fixed with 90	1233
90		277		1333
100		269		1384
110		258		1417
Setting 4: Desired Intensity				
80	−8.23	201	80.21	911
90	−8.44	200	80.79	1031
100	−9.85	202	98.89	1110
110	−11	205	99.12	1097

In setting 1, all three position variables are optimized, including spatial coordinates and orientation. In contrast, in setting 2, only the height is optimized—that is, the light is center and vertically aligned. Counterintuitively, the results show that tilting the light and placing the light slightly off center yield optimal results, providing 4% more cumulative coverage. The comparison of the proposed approach and empirical approach that places the light at the center can be visualized in Figure 16. The explanation is that when the light source is tilted, the AoR interacts with the target surface at an angle, causing the projection shape to elongate. This elongation spreads the light over a larger area while maintaining uniformity in illumination. In addition, placing the light source in the center often results in redundancy, with the highest intensity concentrated at the middle, whereas edge regions receive less light. By tilting and moving the light source off center, the illumination pattern becomes asymmetric, allowing light to be distributed more effectively across the entire area. Even in a symmetrical environment, this redistribution means that more distant areas receive adequate light, increasing the overall effective coverage. Therefore, this simple adjustment—i.e., tilting a light source and positioning it off center—redistributes light more efficiently.

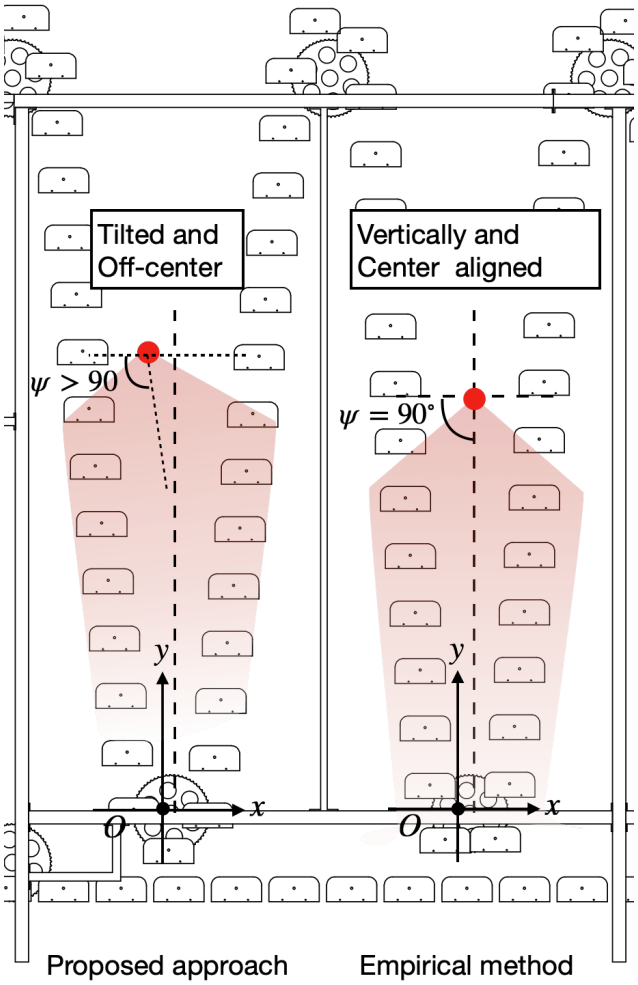

Figure 16. Illustration of difference between proposed and conventional deployment.

In setting 3, the lights are vertically and center aligned, and the height is determined such that the average intensity of each layer has the greatest improvement by a limited uninformed search. Considering average intensity ignores the dynamics in the illumination. In contrast, the proposed approach accurately characterizes the variation of the change in illumination, on which optimization can provide 10% more effective illumination that better meets practical needs.

Setting 4 provides a solution for practical scenarios, where artificial lighting are operated at night and the illuminance on plants must exceed the LCP to ensure proper growth. To evaluate how this requirement influences the deployment of the light source, we set the light's radius to 200. The horizontal coordinate of the light source and pitch angle are adjusted slightly away from intuitive values to optimize overall results. It is important to note that the vertical coordinate of the light source is close to 200, indicating that the light source covering the lower part of the "V" shaped structure yields optimal results. Compared with other settings, the coverage area is drastically reduced and this has to be considered when artificial lights are operated at night.

6.4. Impact on Energy Consumption

Our work primarily focuses on optimizing the positioning of light sources with the pitch angle as the variable, while other conditions are held constant. Although our study does not explicitly evaluate energy consumption, we assert that the optimized light source positions indirectly contribute to more efficient energy usage by enhancing light coverage.

For instance, a 10% improvement in light coverage could potentially reduce the required light-on hours from 10 h to 9 h to achieve the same performance.

However, we realize that optimizations that combine other parameters, including the angle of radiation and the design of the rotating vertical farm, remain an open problem. In future extensions of this work, we aim to incorporate energy consumption analysis alongside the optimization of overall parameter settings to provide a more comprehensive optimization.

7. Conclusions and Future Work

This study established the first framework for designing energy-efficient artificial lighting deployment strategies for stacked vertical farms by incorporating farm structural design, light modeling, and photosynthesis. Based on a theoretical analysis of the beam pattern of lights and the variation in the coverage as the farm layers rotate, we introduced a new criterion, cumulative coverage, which accounts for both light intensity and coverage area. Then, an optimization framework was formulated. A swarm intelligence algorithm, the Differential Evolution algorithm (DE), was used to solve the optimization considering the structural and operational constraints. The proposed approach was compared with two methods, that is, an optimization with variable height only and an empirical method based on uninformed search. We also study the performance of our approach for practical scenarios in which the lights are operated at night. It was found that tilting and placing the light off center yields better results. The results show that the proposed strategy improves light coverage by 4% compared to the optimization with variable height only, and by 10% compared to empirical methods. This study provides insight into improving the efficiency of vertical farming systems.

Future research could explore optimizing farm designs to improve light distribution and overall system efficiency. By refining factors such as light types, electricity usage, material costs, and crop yield, a more comprehensive approach can be developed towards cost-effective and sustainable artificial lighting systems. In addition, variations in natural light due to seasonal and climatic changes were not considered in this paper nor the specific growth requirements of different species. Future work could also focus on tailoring lighting strategies based on the geographic location of the greenhouse and the specific needs of the crops being cultivated. This approach would enable a more precise alignment of artificial light with natural light availability, optimizing plant growth and resource use. Third, future studies could investigate the incorporation of reflective materials into greenhouses. These materials could help redirect and maximize the use of available light, potentially reducing energy consumption and improving the uniformity of light distribution.

Author Contributions: Conceptualization, T.L. and G.Y.; methodology, T.L. and Y.Y.; software, S.T.; simulation, X.X. and H.Z.; result analysis, N.R. and S.S.; T.L. and Y.Y. prepared the manuscript; funding acquisition, G.Y. All authors have read and agreed to the published version of the manuscript.

Funding: This work was supported by Zhejiang Provincial Agriculture "Dual Strength" Project, titled "Rice Seedling Standardization Technology Improvement and New Equipment Demonstration and Promotion", funded by Zhejiang Provincial Department of Agriculture and Rural Affairs.

Data Availability Statement: Data will be made available on request.

Conflicts of Interest: The authors declare no conflicts of interest.

References

1. Nations, U. Population | United Nations—un.org. Available online: https://www.un.org/en/global-issues/population (accessed on 5 November 2024).
2. Nations, U. Urbanization | United Nations—un.org. Available online: https://www.un.org/development/desa/pd/content/urbanization-0 (accessed on 5 November 2024).
3. den Besten, J. Vertical farming development; the Dutch approach. In *Plant Factory Using Artificial Light*; Elsevier: Amsterdam, The Netherlands, 2019; pp. 307–317.
4. Kozai, T.; Niu, G.; Takagaki, M. *Plant Factory: An Indoor Vertical Farming System for Efficient Quality Food Production*; Academic Press: Cambridge, MA, USA, 2019.
5. Banerjee, C.; Adenaeuer, L. Up, up and away! The economics of vertical farming. *J. Agric. Stud.* **2014**, *2*, 40–60. [CrossRef]
6. Paleg, L.; Aspinall, D. Field control of plant growth and development through the laser activation of phytochrome. *Nature* **1970**, *228*, 970–973. [CrossRef] [PubMed]
7. Toth, M.; Kerepesi, I.; Kozma, L.; Klujber, L. Influence of different wave-length laser lights on the carbohydrate metabolism in germinating maize seeds. *Acta Bot. Hung.* **1993**, *38*, 421–430.
8. Podlecœny, J.; Podlecœna, A.; Koper, R. Chilling tolerance of white lupine in early developmental phases–the effect of seed pre-sowing irradiation by laser. In Proceedings of the Workshop Crop Development for the Cool and Wet Regions of Europe, Radzików, Poland, 13–15 March 1997; pp. 13–15.
9. Perveen, R.; Ali, Q.; Ashraf, M.; Al-Qurainy, F.; Jamil, Y.; Raza Ahmad, M. Effects of different doses of low power continuous wave He–Ne laser radiation on some seed thermodynamic and germination parameters, and potential enzymes involved in seed germination of sunflower (*Helianthus annuus* L.). *Photochem. Photobiol.* **2010**, *86*, 1050–1055. [CrossRef] [PubMed]
10. Son, T. Laser activated kenaf. *Tekhnicheskije Kult.* **1990**, *6*, 42–43.
11. Vasilevski, G.; Bosev, D. Results of the effect of the laser light on some vegetables. In *I Balkan Symposium on Vegetables and Potatoes 462*; ISHS: Belgrade, Yugoslavia, 1996; pp. 473–476.
12. Chen, Y.P.; Jia, J.F.; Yue, M. Effect of CO2 laser radiation on physiological tolerance of wheat seedlings exposed to chilling stress. *Photochem. Photobiol.* **2010**, *86*, 600–605. [CrossRef]
13. Koper, R. Pre-sowing laser biostimulation of seeds of cultivated plants and its results in agrotechnics. *Int. Agrophysics* **1994**, *8*, 593–696.
14. Starzycki, M.; Rybiński, W.; Starzycka, E.; Pszczoła, J. Laser light as a physical factor enhancing rapeseed resistance to blackleg disease. *Acta Agrophys.* **2005**, *5*, 441–446.
15. Shaban, N.; Kartalov, P. Effect of laser irradiation of seeds on some physiological processes in cucumbers. *Rasteniev"dni Nauk.* **1988**, *25*, 64–71.
16. Cholakov, D.; Petkova, V. Morphological and physiological characteristics of seedlings caused by laser and gamma irradiation of cucumber seeds. In *II Balkan Symposium on Vegetables and Potatoes 579*; ISHS: Thessaloniki, Greece, 2000; pp. 285–288.
17. Ashrafijou, M.; Noori, S.S.; Darbandi, A.I.; Saghafi, S. Effect of salinity and radiation on proline accumulation in seeds of canola (*Brassica Napus* L.). *Plant Soil Environ.* **2010**, *56*, 312–317. [CrossRef]
18. Abu-Elsaoud, A.M.; Tuleukhanov, S.T.; Abdel-Kader, D.Z. Effect of infra-red laser on wheat (Triticum aestivum) germination. *Int. J. Agric. Res.* **2008**, *3*, 433–438. [CrossRef]
19. Chen, Y.; Xu, D.Q. Two patterns of leaf photosynthetic response to irradiance transition from saturating to limiting one in some plant species. *New Phytol.* **2006**, *169*, 789–798. [CrossRef] [PubMed]
20. Urrestarazu, M.; Nájera, C.; del Mar Gea, M. Effect of the spectral quality and intensity of light-emitting diodes on several horticultural crops. *HortScience* **2016**, *51*, 268–271. [CrossRef]
21. Johkan, M.; Shoji, K.; Goto, F.; Hahida, S.N.; Yoshihara, T. Effect of green light wavelength and intensity on photomorphogenesis and photosynthesis in Lactuca sativa. *Environ. Exp. Bot.* **2012**, *75*, 128–133. [CrossRef]
22. Ke, X.; Yoshida, H.; Hikosaka, S.; Goto, E. Optimization of photosynthetic photon flux density and light quality for increasing radiation-use efficiency in dwarf tomato under LED light at the vegetative growth stage. *Plants* **2021**, *11*, 121. [CrossRef]
23. Linn, R. Experimental Processes for Optimized Lighting Techniques: Enhancing Vertical Farming Crop Growth and Yield Efficiency. Master's Thesis, Kansas State University, Manhattan, KS, USA, 2024.
24. Kaya, A.; Erturk, H.; Yalcin, R.A. Energy efficiency of solar illuminated vertical farms with different illumination strategies. *Energy* **2024**, *307*, 132609. [CrossRef]
25. Olvera-Gonzalez, E.; Escalante-Garcia, N.; Myers, D.; Ampim, P.; Obeng, E.; Alaniz-Lumbreras, D.; Castaño, V. Pulsed led-lighting as an alternative energy savings technique for vertical farms and plant factories. *Energies* **2021**, *14*, 1603. [CrossRef]
26. Yalçın, R.A.; Ertürk, H. Improving crop production in solar illuminated vertical farms using fluorescence coatings. *Biosyst. Eng.* **2020**, *193*, 25–36. [CrossRef]
27. Kim, J.; Kang, W.H.; Son, J.E. Interpretation and evaluation of electrical lighting in plant factories with ray-tracing simulation and 3D plant modeling. *Agronomy* **2020**, *10*, 1545. [CrossRef]

28. Chua, M.D.T.; Adviento, M.R.O.; Lichangco, R.C.A.; Lim, M.A.L. Assessing the Influence of a Rotating Indoor Vertical Farm System on Iceberg Lettuce (*Lactuca sativa* var. *capitata* L.) Growth, Quality, and Yield in Aeroponic Horticulture. In Proceedings of the 5th DLSU Senior High School Research Congress, Laguna, Manila, 27–28 June 2023.
29. Lei, Z.; Chen, X.; Chen, X.; Chai, L. Radial coverage strength for optimization of monocular multicamera deployment. *IEEE/ASME Trans. Mechatronics* **2021**, *26*, 3221–3231. [CrossRef]
30. Chen, X.; Lei, Z.; Yang, Y.; Chai, L. Deployment Optimization of Spotlights for Visual Coverage in Pure Dark Indoor Scene. *IEEE Trans. Ind. Inform.* **2022**, *19*, 8518–8527. [CrossRef]
31. Vegni, A.M.; Biagi, M. Optimal LED placement in indoor VLC networks. *Opt. Express* **2019**, *27*, 8504–8519. [CrossRef] [PubMed]
32. Bi, S.; Zhang, R. Placement Optimization of Energy and Information Access Points in Wireless Powered Communication Networks. *IEEE Trans. Wirel. Commun.* **2016**, *15*, 2351–2364. [CrossRef]
33. Richter, F.; Fehske, A.J.; Fettweis, G.P. Energy efficiency aspects of base station deployment strategies for cellular networks. In Proceedings of the 2009 IEEE 70th Vehicular Technology Conference Fall, Anchorage, AK, USA, 20–23 September 2009; pp. 1–5.
34. Storn, R.; Price, K. Differential evolution–a simple and efficient heuristic for global optimization over continuous spaces. *J. Glob. Optim.* **1997**, *11*, 341–359. [CrossRef]
35. Wang, L.; Deng, F.; Ren, W.J. Shading tolerance in rice is related to better light harvesting and use efficiency and grain filling rate during grain filling period. *Field Crop. Res.* **2015**, *180*, 54–62. [CrossRef]